Strojnícky časopis – *Journal of* MECHANICAL ENGINEERING,
VOL 72 (2022), NO 2, 161 - 172

USE OF LASER METAL DEPOSITION TECHNOLOGY IN ADDITIVE MANUFACTURING OF Ni POWDER MATERIALS

SEJČ Pavol, JAROŠ Ján, VANKO Branislav*

Slovak University of Technology in Bratislava, Faculty of Mechanical Engineering, Institute of Technologies and Materials, Nám. slobody 17, 812 31 Bratislava, Slovakia, e – mail: branislav.vanko@stuba.sk

Abstract: The process parameters of the Laser Metal Deposition technology in the production of simple components made of NiCuBSi type metal powder were verified in this paper. A laser head with a coaxial powder supply and argon gas was used in the production. The powder was welded to a S235J2G3 steel plate. The used parameters (heat input 0.25 kJ.mm^{-1}) enabled the production of samples with a minimum porosity (1.2 %) and without the defects (cold joints, pores) between the weld layers.

KEYWORDS: additive manufacturing, Laser Metal Deposition, self-fluxing NiCuBSi metal powder

1 Introduction

Additive manufacturing (AM) currently has a relatively wide application in technical practice [1]. Its basic characteristic is the gradual layering of the applied material into the shape of the final product. In this way, it is currently possible to produce components from plastics, metal, and ceramic materials [1-9].

The feedstock material intended for AM can have different shapes - wires, tapes or powders are used. For wire applications, the main dimensional parameter is diameter, for strips it is width and thickness. For powder applications, it is necessary to consider not only the shape of the particles and their mean size (D_{50}), but also the particle size distribution.

ASTM standard F2792 divides AM metal components into two basic groups: Directed Energy Deposition (DED) and Powder Bed Fusion (PBF) [10]. In the application of metallic materials, powerful heat sources are required for AM, such as Gas Metal Arc (GMA), Plasma Arc (PA), Laser (L) or Electron Beam (EB). Of these sources, the laser beam currently has the widest application [11-13].

In the PBF process, a heat source is used to selectively melt and bond a layer of metal powders on a powder bed. In PBF-L, the powder applied in a thin layer is selectively (in contours) heated by a laser beam. The movement is controlled by CNC for each layer. This process is repeated layer by layer until the desired 3D shape is finally achieved. In the PBF group, Selective Laser Melting (SLM) is a commonly applied technology using precisely controlled laser beam [14-17].

In the DED process, production is based on the supply of metal powders or wires to a melt generated by an intense heat source. In the case of powder cladding, the feedstock material (powder) is fed from the hopper (single-nozzle or co-axial) into the laser beam. The heat melts the powder, while the contours of the applied layer are ensured by the 2D movement of the laser head. The thickness of the layer will be proportional to the amount of feed and molten powder material. Powder-based DED technology using a laser as an energy source is also called Laser Metal Deposition (LMD) [1, 18-26].

DOI: 10.2478/scjme-2022-0026, Print ISSN 0039-2472, On-line ISSN 2450-5471

Various types of metal powders based on steels as well as non-ferrous metals are currently used in LMD technology [27-29]. There are materials made of pure Ni [30], superalloys [31, 32] or self-fluxing alloys [33, 34] in the group of Ni-based powders.

Ni-based self-fluxing alloy powders are primarily intended for thermal spraying during renovations or the formation of tribological coatings [35, 36]. Higher hardness layers made of NiCrSiB type powders show a high wear resistance, which is ensured by Cr_xC_y type carbides or complex carbonitrides $(Ni,Cr)_x(C,N)_y$. On the other hand, NiCuSiC type powders show good resistance to temperature changes, excellent resistance to seawater and are suitable for surface treatment of gray cast iron products. NiCuSiC and NiFeSiB powders with lower hardness also serve as a tough substrate for the application of composite materials, e.g. type NiFeSiB + WC or NiCuSiB + WC [35-38].

2 Experiment

The aim of the work was to assess the suitability of the use of nickel powder NiCuBSi type for the additive manufacturing of components by LMD technology. The following were assessed on simple shape samples:

1. the effect of heat input by multi-pass cladding on the formation of the joint between the 1st layer and the base material and on the bonds between the deposited layers,

2. shape changes caused by heat-induced stresses and changes in the speed of the laser head,

3. dimensional increments after making individual deposited layers,

4. macrostructures of AM sample for defects detection (lack of fusion, incomplete penetration, porosity),

5. hardness,

6. phase analysis of metal structure.

A NiCuBSi type self-fluxing alloy powder NP16 was used for weld cladding, in which B ensures the dissolution of surface oxides and, together with Si, lowers the melting temperature, improves the flowability and wettability of the melt. The material used is characterized by lower hardness and good plastic properties. The weld will thus be resistant to delayed hot cracks and suitable for subsequent machining. The globular shape of the particles will have a positive effect on the feeding of the powder into the welding head. The chemical composition of the powder NP16 is in Table 1, the other selected properties are in Table 2.

Table 1 Chemical composition of the powder NP16 [38]

Chemical element	C	Si	B	Fe	Cu	Cr	Ni
Weight concentration of the element (wt. %)	max. 0.25	max. 5.0	max. 3.0	max. 5.0	max. 20.0	-	rest

Table 2 Selected properties of the powder NP16 [38]

Hardness HV	Melting point (°C)	Grain size (μm)	Grain shape	Apparent density ($g.cm^{-3}$)	Flowability (s/50g)
180÷235	1010	<100+5	spheroidal	5.0	14

Two models of simple test specimens were designed to solve the problems (Figs. 1 and 2). The first model shown in Fig. 1, represented a linear layering into the final shape of a simple straight walls. The model was used to evaluate the shape and dimensional properties, macro and microstructure of AM product. The designed wall length was 200 mm, height 12 mm, and

thickness 4 mm. The second model, shown in Fig. 2, represented the layering into a regular octagon. This model was used to analyse the movements of an industrial robot in the production of a more complex shape. When changing the direction of movement of the laser head at the edges (corners) of the octagonal prism, the speed of the head slowed down to a short stop. The model was therefore used mainly to evaluate the effect of changes in the speed of the laser head on the shape and dimensional deviations of the prepared sample. The designed length of the octagon wall was 26 mm, the distance between the two parallel walls 63 mm, heigh of the wall 12 mm, and thickness 4 mm.

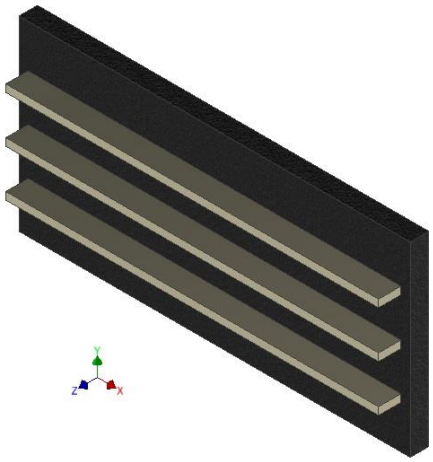


Fig. 1 Model with simple straight walls

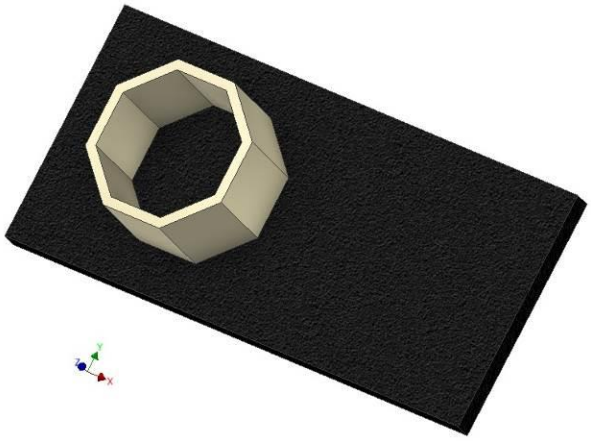


Fig. 2 Model with octagonal prism

Weld cladding was carried out on base plates measuring 210x100x10 (mm) made of steel S235J2G3 (1.0116). Prior to welding, the surface of the plates was ground and degreased.

Prior to the experiments, the powder was dried at 110 °C for 2 hours. The dried and cooled powder was then poured into the powder feeder hopper at the laser station. Argon was used as a carrying and shielding gas during the manufacturing process.

The technical equipment for laser beam welding consisted of:

- fibre laser IPG Photonics YLS - 6000 (wavelength: 1070 nm, power: 6 kW),
- six-axis industrial robot KUKA KR16-2,
- KUKA KR C4 robot controls,
- laser welding head with co-axial powder feeding through 4 nozzles,
- CastoDyn EP powder feeder hopper,
- worktable with two rotary welding positioners,
- laser workplace for class 4 laser with flue gas extraction,
- two-channel thermometer with thermocouple.

A laser head with a coaxial powder supply was used for weld cladding. The technical solution of laser beam welding is shown in Fig. 3. The parameters related to the focusing of the laser beam and the heating of the supplied powder are shown in Fig. 4. The process parameters for the production of test specimens are in Table 3.

The laser beam was focused 30 mm above the base material (substrate). It thus created a spot with a diameter of 4 mm on the substrate surface. The nozzles for the powder supply were 20 mm from the substrate. A cone of powder entrained in argon entered the laser beam at a distance p_d from the substrate (Fig. 4) - at this length, the powder was heated by the laser beam.

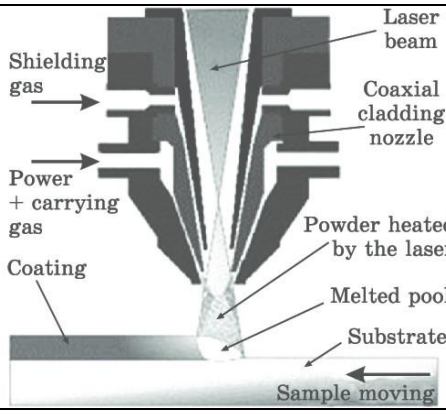


Fig. 3 Principle of laser beam welding with co-axial powder nozzle feeding [26]

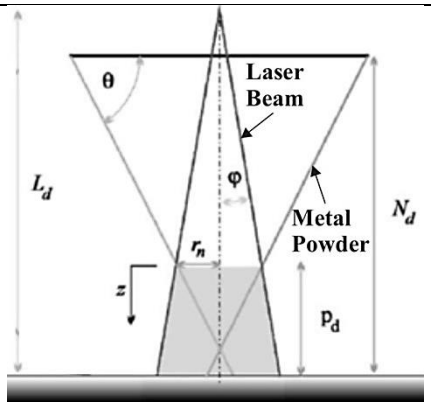


Fig. 4 Laser beam heating geometry [21]

Table 3 Process parameters for the production of test specimens (Fig. 4)

Parameter	Symbol	Value
Laser beam power [W]	P	2000
Cladding speed [mm.s^{-1}] *	v	8
Spot beam diameter on substrate [mm]	d	4
Beam focus distance from substrate [mm]	L_d	30
Nozzle distance from substrate [mm]	N_d	20
Powder feed per minute [g.min^{-1}]	F	27
Carrying gas flow per minute [l.min^{-1}]	h	5
Shielding gas flow per minute [l.min^{-1}]	o	15
Specific heat input [kJ.mm^{-1}]	Q	0.25
Power density [W.cm^{-2}]	I	15915

* The constant cladding speed (speed of the laser head) was applied only for a model with simple straight walls. During the production of the octagonal prism, the cladding speed at the edges was significantly reduced.

When welding nickel and nickel alloys, preheating of the substrate is generally not used and the temperature of the weld metal just before the start of welding of the next layer in multi-layer welds, so-called interpass temperature, is limited to max. 100 °C [39]. Exceeding the interpass temperature can adversely affect the mechanical properties of the weld metal, so it was necessary to observe this condition in the experiment. When forming multi-layer welds without cooling, the temperature increases with each layer until a critical state begins, when a new layer of weld starts to flow. At elevated temperatures, there is also an excessive increase in grain size in the Heat Affected Zone (HAZ) under the new weld. The coarse-grained structure adversely affects the resulting strength of the finished AM product.

In the presented work, the measurement of interpass temperature by contact method (thermocouple) was always carried out at the beginning of the welding of a specific layer.

3 Results

Figs. 5 and 6 show samples after linear overlapping of layers in simple straight walls. As can be seen at first glance, during production, the heat-induced tensile stresses generated tore the deposited layers off the substrate. This fact resulted from insufficient metallurgical bonding between the 1st deposited layer and the substrate.



Fig. 5 Sample with simple straight walls

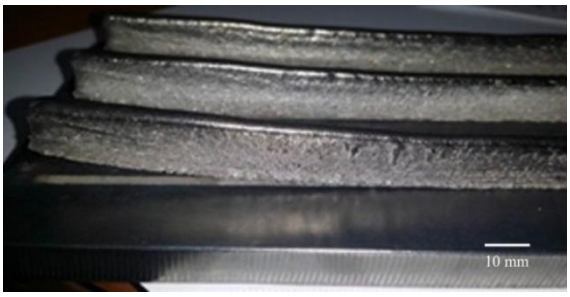


Fig. 6 Detail of tearing and bending of walls

The cause of the rupture was a very low heat input (0.25 kJ.mm^{-1}), which was insufficient for the metallurgical joint of the nickel weld and the steel plate. On the other hand, the heat input used was sufficient to form metallurgical bonds between the deposited layers (Fig. 7). No lack of fusion or other defects such as hot cracks were not observed on the cross section at the interface of the layers. Several solutions are offered to solve the problem of insufficient joint strength between the substrate and the 1st deposited layer:

1. application of the 1st deposited layer with higher heat input (use higher laser beam power),
2. application of the 1st deposited layer on the preheated substrate,
3. change in the chemical composition of the substrate.

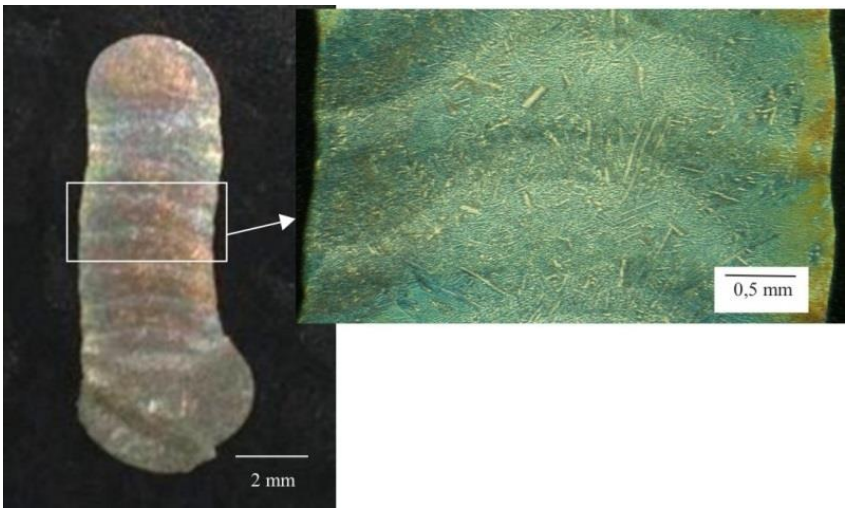


Fig. 7 Cross section of a simple straight wall

Table 4 shows the growth of a simple straight wall and monitoring the interpass temperature. The largest height increment (2 mm) was recorded when creating the 1st deposited layer. However, the large heat dissipation into the substrate did not ensure a metallurgical joint between the 1st deposited layer and the substrate. During wall formation, its growth stabilized at 0.66 mm per layer after layer 7. The maximum value of the interpass temperature 100 °C was observed during the production of the test sample.

Fig. 8 shows a sample of a regular octagonal prism. The total height of the model after producing of 10 deposited layers was 12.6 mm. In this case, the deposited layers were torn off from the substrate too. In a more detailed analysis, only a slight excess of the upper layer at the edges (corners) of the octagonal prism is evident. The cause of the excess is a reduction in the speed of the laser head in corners without correcting the amount of powder fed. However, this excess did not have a significant effect on the shape of the prism. Table 5 shows the creation of an octagonal prism and monitoring the interpass temperature. Again, a decreasing increase in the height of the wall was recorded from the 1st to the last deposited layer, while after the 7th deposited layer the height increments stabilized at 0.77 mm.

Table 4 Wall building when creating a simple straight wall

Layer number	Total wall height (mm)	Interpass temperature (°C)	Height increment per layer (mm)
1	2	20	2
2	3	31	1
3	4.6	38	1.6
4	6.1	41	1.5
5, 6, 7	9.8	42	1.23
8, 9, 10	11.8	88	0.66

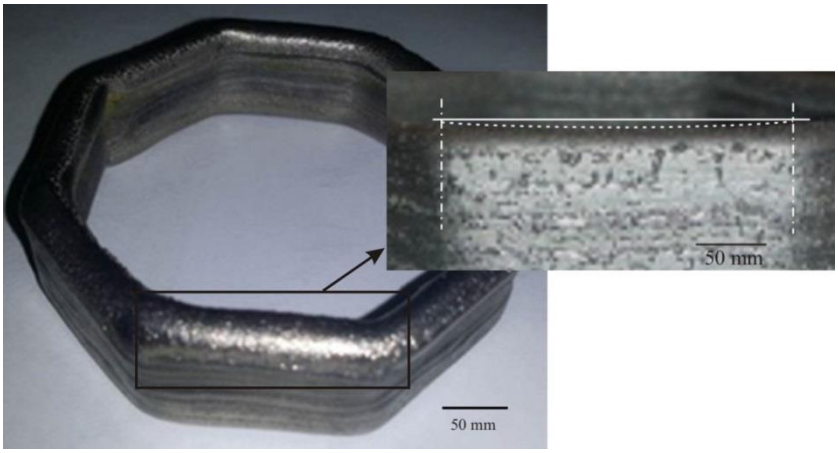


Fig. 8 Sample of an octagonal prism with a detail of a slight excess at the edges

Table 5 Wall building when creating of an octagonal prism

Layer number	Total wall height (mm)	Interpass temperature (°C)	Height increment per layer (mm)
1	1.8	20	1.8
2, 3, 4	6.0	35	1.4
5, 6, 7	10.3	80	1.43
8, 9, 10	12.6	82	0.77

The LMD process parameters were designed for an average wall thickness of 4 mm. The real measured data of wall thickness (width of the deposited layers) at different distances from the substrate in the production of a simple straight wall and an octagonal prism are shown in Fig. 9. From the obtained data it can be stated that the nearly constant width of the deposited layer occurred after the application of the 4th deposited layer in the production of a simple straight wall, or 3rd deposited layer in the production of an octagonal prism. A larger amount of applied material in the production of the octagonal prism is related to changes (decrease in the speed of the laser head) in the formation of corner sections (edges) without correction of the amount of powder supply.

The total porosity of the AM samples was evaluated by image analysis of cross-sections of walls (Figs. 10 and 11) using the software ImageJ. As can be seen, the macrostructure of the simple straight wall as well as the octagonal prism was homogeneous, without the occurrence of lacks of fusion and with minimal porosity. In both cases the porosity was at the level of 1.2 %.

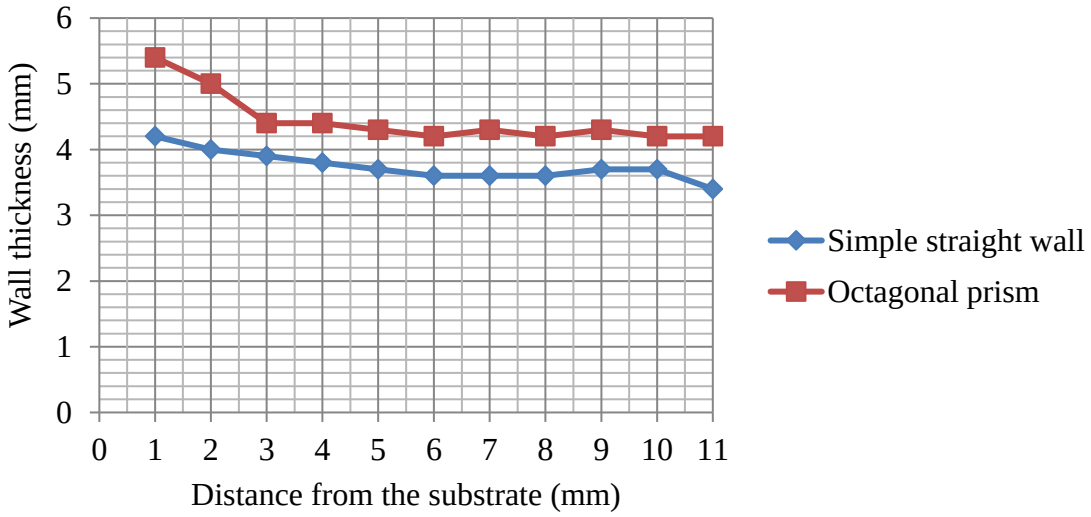


Fig. 9 Changes in wall thickness (width of the deposited layers) in the production of a simple straight wall and an octagonal prism at different distances from the substrate

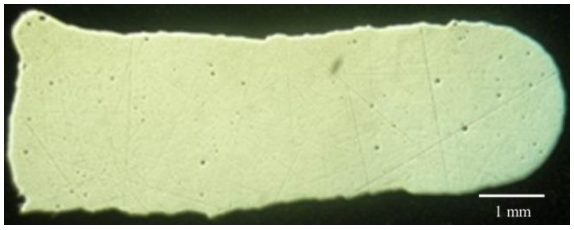


Fig. 10 Macrostructure of a cross-section of a simple straight wall

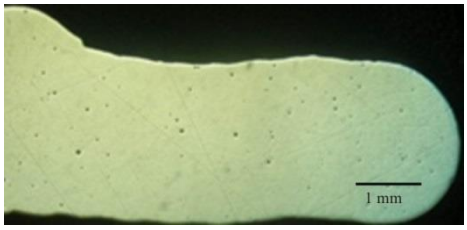


Fig. 11 Macrostructure of a cross-section of an octagonal prism wall

The homogenenity of the macrostructure of the deposited layers in the production of a simple straight wall is also confirmed by the hardness measurement (Fig. 12). The resulting hardness of the test sample was 278.2 ± 9.9 HV30 with a relative measurement error of 3.56 %. A higher loading force during hardness measurement (HV30) was chosen to eliminate the influence of structural inhomogeneities.

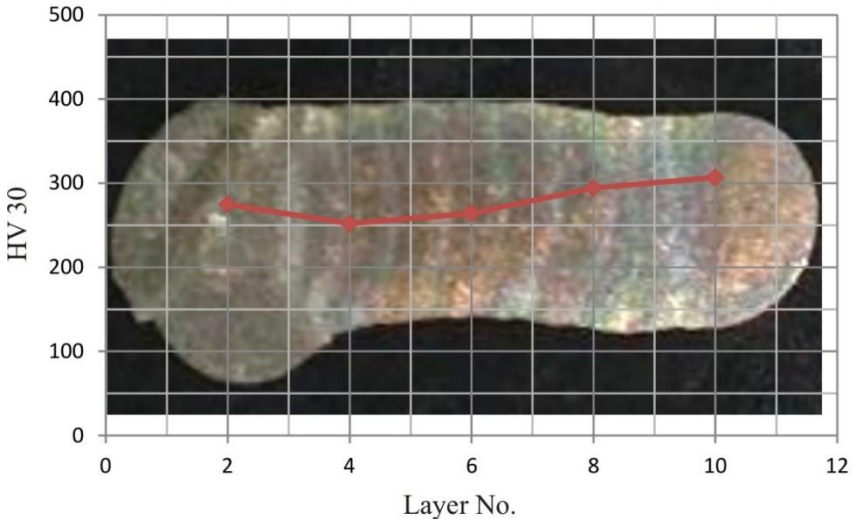


Fig. 12 The course of hardness of deposited layers in a simple straight wall

These findings confirm the appropriate choice of LMD process parameters in terms of melting the powder as well as the metallurgical bonding between deposited layers, which

formed the final dimension of the model with simple straight walls and the model with octagonal prism.

It is known that, unlike conventional processes such as casting and welding, AM processes are characterized by high cooling rates and repeated heating and cooling cycles, which significantly affect the development of the microstructure of the deposited layers [1]. In our case, the microstructure consisted, depending on the thermal influence, of columnar and equiaxed dendrites (Fig. 13). Dendrites were formed by a solid solution of Si, Fe, Cu in γ-Ni and interdendritic spaces were formed by an eutectic (Fig. 14) - a mixture of solid solution and borides Ni_3B or carbo-borides $Ni_3(B,C)$, which confirms the EDS analysis of selected areas (Table 6).

Previous research has shown that in LMD technology, the heat treatment of the substrate through homogenization annealing eliminates the anisotropy of the material [27]. In our case, the structural changes resulting from the heat treatment consisting of repeated heating and cooling cycles were also reflected by a slight decrease in the hardness of the lower deposited layers (Fig. 12).

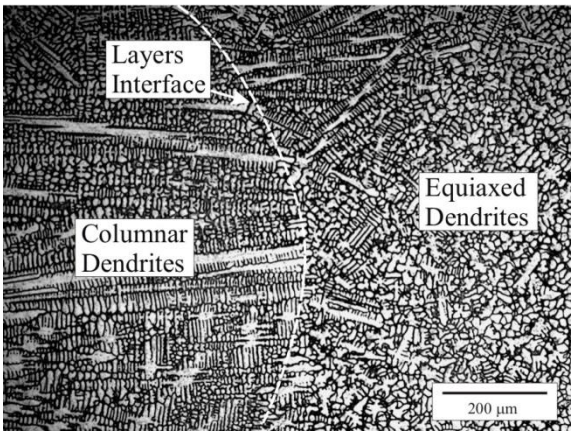


Fig. 13 Microstructure of a simple straight wall (light microscopy)

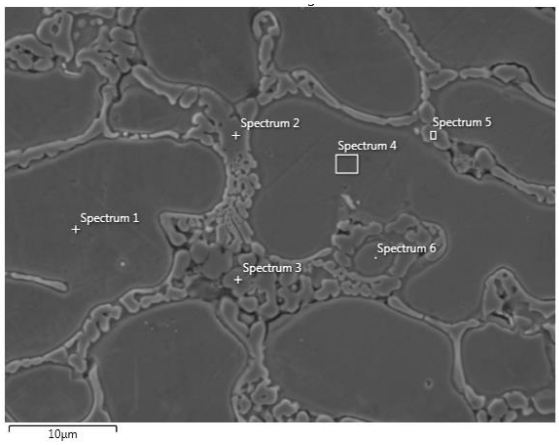


Fig. 14 Microstructure of a simple straight wall (SEM) with areas marked for EDS analysis

Table 6 EDS analysis of selected areas (see Fig. 14)

Selected area	Chemical element (at. %)					
	B	C	Si	Fe	Ni	Cu
Spectrum 1	15.88	17.12	3.05	0.23	50.35	13.36
Spectrum 2	34.91	17.90	-	-	45.47	1.72
Spectrum 3	35.16	14.13	0.19	-	48.61	1.91
Spectrum 4	12.28	19.25	3.37	-	50.83	14.26
Spectrum 5	30.83	17.08	0.25	-	49.77	2.08
Spectrum 6	-	18.70	4.30	-	58.94	18.07

CONCLUSION

The work is focused on verifying selected process parameters of the additive manufacturing technology Laser Metal Deposition (LMD) in the production of simple samples (simple straight wall and octagonal prism) from metal powder NiCuBSi type. The feedstock material was joined to a S235J2G3 steel plate. From the achieved results can be drawn the following conclusions:

1. The low heat input of the laser (0.25 kJ.mm^{-1}) did not ensure a permanent metallurgical joint of the 1st deposited layer of Ni-alloy powder with the steel plate. The heat-induced stress generated during the production of the simple straight wall and the octagonal prism caused the layer to tear off the steel plate.
2. The heat input used was sufficient to create a metallurgical joint between the deposited layers. The process parameters enabled the production of samples with a minimum porosity (1.2 %) without the occurrence of defects (lacks of fusion, cracks).
3. After applying the 3rd deposited layer (octagonal prism) or 4th layer (simple straight wall) only minimal changes in the width of the samples were recorded. As well as the reduction of the speed of the laser head at the corners of the octagonal prism had only a minimal effect on the shape and dimensional deviations.
4. The microstructure of the produced AM samples consisted of a solid solution of Si, Fe, Cu in γ-Ni and eutectics - a mechanical mixture of solid solution and borides Ni_3B or carbo-borides $Ni_3(B,C)$ with an average hardness of 278 HV30.

ACKNOWLEDGMENTS

The results given in this paper were obtained with support of the UVP STU v Bratislave, project ITMS 26240220084.

REFERENCES

[1] DebRoy, T., Wei, H. L., Zuback, J. S., Mukherjee, T., Elmer, J.W., Milewski, J. O., Beese, A. M., Wilson-Heid, A., De, A., Zhang, W. "Additive manufacturing of metallic components – Process, structure and properties", Progress in Materials Science 92, pp. 112 – 224, **2018**. DOI: 10.1016/j.pmatsci.2017.10.001

[2] Magerramova, L., Volkov, M., Svinareva, M., Siversky, A. "The use of additive technologies to create lightweight parts for gas turbine engine compressors", In: Proceedings of ASME Turbo Expo 2018 Turbomachinery Technical Conference and Exposition GT2018, Oslo, Norway, pp. 1 – 7, **2018**.

[3] Hae-Sung, Y., Jang-Yeob, L., Hyung-Soo, K., Min-Soo, K., Eun-Seob, K., Yong-Jun, S., Won-Shik, Ch., Sung-Hoon, A. "A Comparison of Energy Consumption in Bulk Forming, Subtractive, and Additive Processes: Review and Case Study", International Journal of Precision Engineering and Manufacturing-Green Technology 1 (3), pp. 261 – 279, **2014**. DOI: 10.1007/s40684-014-0033-0

[4] Thompson, M. K., Moroni, G., Vaneker, T., Fadel, G., Campbell, R. I., Gibson, I., Bernard, A., Schulz, J., Graf, P., Ahuja, B., Martina, F. "Design for Additive Manufacturing: Trends, Opportunities, Considerations and Constraints", CIRP Annals – Manufacturing Technology 65 (2), pp. 737 – 760, **2016**. DOI: 10.1016/j.cirp.2016.05.004

[5] Herzog, D., Seyda, V., Wycisk, E., Emmelmann, C. "Additive manufacturing of metals", Acta Materialia 117, pp. 371 – 392, **2016**. DOI: 10.1016/j.actamat.2016.07.019

[6] Castro e Costa, E., Pinto Duarte, J., Bártolo, P. "A review of additive manufacturing for ceramic production", Rapid Prototyping Journal, 23/5, pp. 954 – 963, 2017. DOI: 10.1108/RPJ-09-2015-0128

[7] Tuominen, J., Kaubisch, M., Thieme, S., Nakki, J., Nowotny, S., Vuoristo, P. "Laser strip cladding for large area metal deposition", Additive Manufacturing 27, pp. 208 – 216, **2019**. DOI: 10.1016/j.addma.2019.01.008

[8] Handrik M., Vaško M., Majko J., Sága M., Dorčiak F. "Influence of the Shape of the Test Specimen Produced by 3D Printing on the Stress Distribution in the Matrix and in Long Reinforcing Fibers", Strojnícky časopis – Journal of Mechanical Engineering 69 (3), pp. 61 – 68, **2019**. DOI: 10.2478/scjme-2019-0030

[9] Dimić A., Mišković Ž., Mitrović R., Ristivojević M., Stamenić Z., Danko J., Bucha J., Milesich T. "The Influence of Material on the Operational Characteristics of Spur Gears Manufactured by the 3D Printing Technology", Strojnícky časopis – Journal of Mechanical Engineering 68 (3), pp. 261 – 270, **2018**. DOI: 10.2478/scjme-2018-0039

[10] ASTM F2792-12. "Standard Terminology for Additive Manufacturing Technologies", **2012**.

[11] Murr, L. E., Gaytan, S. M., Ramirez, D. A., Martinez, E., Hernandez, J., Amato, K. N., Shindo, P. W., Medina, F. R., Wicker, R. B. "Metal Fabrication by Additive Manufacturing Using Laser and Electron Beam Melting Technologies", Journal of Material Science Technology 28 (1), pp. 1 – 14, **2012**.

[12] Schmidt, M., Merklein, M., Bourell, D., Dimitrov, D., Hausotte, T., Wegener, K., Overmeyer, L., Vollertsen, F., Levy, G. N. "Laser based additive manufacturing in industry and academia", CIRP Annals - Manufacturing Technology 66, pp. 561 – 583, **2017**. DOI: 10.1016/j.cirp.2017.05.011

[13] Lei Y., Yitao Ch., Frank L. "Additive manufacturing of functionally graded metallic materials using laser metal deposition", Additive Manufacturing 31, pp. 1 – 11, **2020**. DOI: 10.1016/j.addma.2019.100901

[14] Kruth, J. P., Wang, X., Laoui, T., Froyen, L. "Lasers and materials in selective laser sintering", Assembly Automation 23 (4), pp. 357 – 371, **2003**. DOI: 10.1108/01445150310698652

[15] "Velcome to SLM Solutions". [online] Available at: www.slm-solutions.com [Accessed: 14-12-**2021**].

[16] Yap, C. Y., Chua, C. K., Dong, Z. L., Liu, Z. H., Zhang, D. Q., Loh, L. E., Sing, S. L. "Review of selective laser melting: Materials and applications", Applied Physics Reviews 2, 041101, **2015**. DOI: 10.1063/1.4935926

[17] Atwood, C., Griffith, M., Harwell, L., Schlienger E., Ensz M., Smugeresky J., Romero T., Greene D., Reckaway D. "Laser engineered net shaping (LENS™): A tool for direct fabrication of metal parts". In: 17th International Congress on Applications of Lasers and Elector-Optics; Orlando, USA, **1998**. DOI: 10.2351/1.5059147

[18] Akbari, M., Kovacevic, R. "An investigation on mechanical and microstructural properties of 316LSi parts fabricated by a robotized laser/wire direct metal deposition system", Additive Manufacturing 23, pp. 487 – 497, **2018**. DOI: 10.1016/j.addma.2018.08.031

[19] Elif Karayel, K., Yahya Bozkurtb, Y. "Additive manufacturing method and different welding applications", Journal of Materials Research and Technology 9 (5), pp. 11424 – 11438, **2020**. DOI: 10.1016/j.jmrt.2020.08.039

[20] Zhanga, K., Liua, W., Shanga, X. "Research on the processing experiments of laser metal deposition shaping", Optics & Laser Technology 39, pp. 549 – 557, **2007**. DOI: 10.1016/j.optlastec.2005.10.009

[21] de Oliveira, U., Ocelík, V., De Hosson, J. Th. M. "Analysis of coaxial laser cladding processing conditions", Surface & Coatings Technology 197, pp. 127 – 136, **2005**. DOI: 10.1016/j.surfcoat.2004.06.029

[22] Arnold, J., Volz, R. "Laser Powder Technology for Cladding and Welding", Journal of Thermal Spray Technology 8 (2), pp. 243 – 248, **1999**.

[23] Zhenglong, L., Kezhao, Z., Heng, Z., Longchang, N., Yanbin, Ch. "A comparative study of microstructure and tensile properties of Ti2AlNbjoints prepared by laser welding and laser-additive welding with theaddition offiller powder". Journal of Materials Processing Technology 255, pp. 477 – 487, **2018**. DOI: 10.1016/j.jmatprotec.2017.12.044

[24] Caiazzo, F., Alfieri, V. "Optimization of laser beam welding of steel parts made by additive manufacturing", The International Journal of Advanced Manufacturing Technology 114, pp. 3123 – 3136, **2021**. DOI: 10.1007/s00170-021-07039-w

[25] Danielewski, H., Antoszewski, B. "Properties of Laser Additive Deposited Metallic", Open Engineering 10, pp. 484 – 490, **2020**. DOI: 10.1515/eng-2020-0046

[26] Geng, Y., Konovalov, S. V., Chen, X. "Research Status and Application of the High-Entropy and Traditional Alloys Fabricated via the Laser Cladding ", Progress in Physics of Metals 21 (1), pp. 26 – 45, **2020**. DOI: 10.15407/ufm.21.01.026

[27] Mahamood, R. M. "Laser metal deposition process of metals, alloys, and composite materials", Springer, Cham, Switzerland, **2018**. DOI: 10.1007/978-3-319-64985-6

[28] Kai, Z., Shijie, W., Weijun, L., Xiaofeng, S. "Characterization of stainless steel parts by Laser Metal Deposition", Materials and Design 55, pp. 104 – 119, **2014**. DOI: 10.1016/j.matdes.2013.09.006

[29] Awd, M., Tenkamp, J., Hirtler, M., Siddique, S., Bambach, M, Walther, F. "Comparison of Microstructure and Mechanical Properties of Scalmalloy® Produced by Selective Laser Melting and Laser Metal Deposition", Materials 11 (1), pp. 1 – 17, **2018**. DOI: 10.3390/ma11010017

[30] Chor, Y. Y., Hongyi, K. T., Zhenglin, D., Chee, K. Ch. "Selective laser melting of nickel powder", Rapid Prototyping Journal 23(4), pp. 750 – 757, **2017**. DOI: 10.1108/RPJ-01-2016-0006

[31] Babu, S. S., Raghavan, N., Raplee, J., Foster, S. J., Frederick, C., Haines, M., Dinwiddie, R., Kirka, M. K., Plotkowski, A., Lee, Y., Dehoff, R. R. "Additive Manufacturing of Nickel Superalloys: Opportunities for Innovation and Challenges Related to Qualification", Metallurgical and Materials Transactions A 49A, pp. 3764 – 3780, **2018**. DOI: 10.1007/s11661-018-4702-4

[32] Liang, Y. J., Cheng X., Li J., Wang, H. M. "Microstructural control during laser additive manufacturing of single-crystalnickel-base superalloys: New processing–microstructure maps involving powder feeding", Materials & Design 130, pp. 197 – 207, **2017**. DOI: 10.1016/j.matdes.2017.05.066

[33] Shishkovsky, I., Kakovkina, N., Sherbakof, V. "Mechanical properties of NiCrBSi self-fluxing alloy after LPBF with additional heating", Procedia CIRP 94, pp. 217 – 221, **2020**. DOI: 10.1016/j.procir.2020.09.041

[34] Hu, D., Liu, Y., Chen, H., Liu, J., Wang, M., Deng, L. "Microstructure and properties of Ta-reinforced NiCuBSi + WC composite coating deposited on 5Cr5MoSiV1 steel

substrate by laser cladding", Optics & Laser Technology 142, 107210, pp. 1 – 10, **2021**. DOI: 10.1016/j.optlastec.2021.107210

[35] Karimi, M. R., Salimijazi, H. R., Golozar, M. A. "Effects of remelting processes on porosity of NiCrBSi flame sprayed coatings", Surface Engineering 32 (3), pp. 238 – 243, **2015**. DOI: 10.1179/1743294415Y.0000000107

[36] Vencl, A., Katavić, B., Marković, D., Ristić, M., Gligorijević, B. "The Tribological Performance of Hardfaced Thermal Sprayed Coatings", Tribology in Industry 37 (3), pp. 320 – 329, **2015**.

[37] Iždinská, Z., Nasher, A., Iždinský, K. "The Structure and Mechanical Properties of NiCrBSi Coatings Prepared by Laser beam Cladding", Materials Engineering 17 (1), pp. 11 – 16, **2010**.

[38] "Kovové prášky". [online] http://www.vuz.sk/uploads/wysiwyg/katal%C3%B3gy/10_Kovove_prasky.pdf [Accessed: 15-12-**2021**].

[39] Caron, J. L., Sowards, J. W. "6.09 - Weldability of Nickel-Base Alloys", In: Hashmi S., Van Tyne Ch. J., Gilmar G. F., Yilbas B. Comprehensive Materials Processing 6: Welding and Bonding technologies. 1st edition, Elsevier, pp. 50 – 75, **2014**. DOI: 10.1016/B978-0-08-096532-1.00615-4